

Shear stiffness of headed studs on structural behaviors of steel-concrete composite girders

Jun He^{1,2}, Zhaofei Lin³, Yuqing Liu^{*4}, Xiaoqing Xu⁵, Haohui Xin^{6,7} and Sihao Wang⁴

¹School of Civil Engineering, Changsha University of Science and Technology, Hunan, China

²Institute for Infrastructure and Environment, Heriot-Watt University, Edinburgh, UK

³Country Garden, Guangdong, China

⁴Department of Bridge Engineering, Tongji University, Shanghai, China

⁵School of Civil Engineering, Chongqing University, Chongqing, China

⁶School of Human Settlements and Civil Engineering, Xi'an Jiaotong University, Xi'an, China

⁷Faculty of Geoscience and Engineering, Delft University of Technology, The Netherlands

(Received January 27, 2020, Revised July 30, 2020, Accepted August 14, 2020)

Abstract. Steel-concrete composite structures have been extensively used in building, bridges, and other civil engineering infrastructure. Shear stud connectors between steel and concrete are essential in composite members to guarantee the effectiveness of their behavior in terms of strength and deformability. This study focuses on investigating the shear stiffness of headed studs embedded in several types of concrete with wide range of compressive strength, and their effects on the elastic behavior of steel-concrete composite girders were evaluated. Firstly, totally 206 monotonic push-out tests from the literature were reviewed to investigate the shear stiffness of headed studs embedded in various types of concrete (NC, HPC, UHPC etc.). Shear stiffness of studs is defined as the secant stiffness of the load-slip curve at $0.5V_{us}$, and a formulation for predicting defined shear stiffness in elastic state was proposed, indicating that the stud diameter and the elastic modulus of steel and concrete are the main factors. And the shear stiffness predicted by the new formula agree well with test results for studs with a diameter ranging from 10 to 30 mm in the concrete with compressive strength ranging from 22.0 to 200.0MPa. Then, the effects of shear stiffness on the elastic behaviors of composite girders with different sizes and under different loading conditions were analyzed, the equations for calculating the stress and deformation of simply supported composite girders considering the influence of connection's shear stiffness were derived under different loading conditions using classical linear partial-interaction theory. As the increasing of shear stiffness, the stress and deflection at the most unfavorable section under partial connected condition tend to be those under full connected condition, but the approaching speed decreases gradually. Finally, the connector's shear stiffness was recommended for fully connection in composite girders with different dimensions under different loading conditions. The findings from present study may provide a reference for the prediction of shear stiffness for headed studs and the elastic design of steel-concrete composite girder.

Keywords: composite girder; headed studs; shear stiffness; elastic behaviors; push-out test

1. Introduction

Steel-concrete composite structures have been extensively used in building, bridges, and other civil engineering infrastructure, making an effective utilization of concrete in the compression zone and steel in the tension counterpart, offering several advantages. The primary one is the high strength-to-weight ratio as compared to conventional reinforced concrete (RC) structures. They also offer greater flexural stiffness, speedier and more flexible construction, ease of retrofitting and repair, and higher durability (Chen 2005, He *et al.* 2010, 2017, 2020a, b, Lin *et al.* 2014a, b).

In steel-concrete composite structures, shear connectors between steel and concrete (e.g., angles, channel sections, headed studs, perforated ribs) are essential in all composite

members in order to guarantee the effectiveness of their behavior in terms of strength and deformability. Those connectors, located in the steel-concrete interface, must be able to effectively transfer the stresses occurring between both materials (Lam and El-Lobody 2005, Colajanni *et al.* 2014, He *et al.* 2014, 2019).

Headed stud connector is one of the most popular shear connectors owing to its simple and quick installation using a stud-welding gun and superior ductility. Headed steel studs welded to the flange of the steel beam and embedded in concrete solid slab, or in composite slab using profiled steel sheeting, have been the most common procedure to transfer longitudinal shear forces between the steel beam and concrete slab in composite girders (Oehlers and Coughlan 1986, An and Cederwall 1996, Lee *et al.* 2005, Pallarés and Hajjar 2010, Shim *et al.* 2004, Xue *et al.* 2012, Suwaed and Karavasilis 2018).

Recently a number of researchers have focused on the different aspects of headed stud connectors. An extensive experimental research on shear behaviors of stud connectors under static or cyclic loading (Gattesco and Giuriani 1997,

*Corresponding author, Professor
E-mail: yql@tongji.edu.cn; hejun@csust.edu.cn

Shim *et al.* 2004, Civjan and Singh 2003) and fatigue loading (Dogan and Roberts 2012, Lee *et al.* 2005) were carried out, considering the influence of concrete strength and types (An and Cederwall 1996, Valente and Cruz 2009, Kim *et al.* 2015; Han *et al.* 2017), such as crumb rubber concrete (Han *et al.* 2015, 2017), high-performance concrete (HPC) (Cao *et al.* 2017, Kim *et al.* 2015, Tian and Du 2016), steel fiber-reinforced cementitious composites (SFRCCs) (Luo *et al.* 2016, Xu *et al.* 2017); the diameter of studs (Badie *et al.* 2002, Shim *et al.* 2004), the biaxial loading effect on group studs (Xu *et al.* 2018, Lin *et al.* 2014), the quantity of studs (Xue *et al.* 2008, Xue *et al.* 2012, Spremic *et al.* 2013, 2018) and the restrained conditions and loading conditions (Lin *et al.* 2015, 2016). These researches indicate that the shear capacity of studs depends on many factors, including the material and diameter of the stud itself and properties of the surrounding concrete slab, and these factors are considered for predicting shear capacity of stud connectors in several national design codes (AISC, 2005; BS5400, 1978; CEN-Eurocode 4, 2005; AASHTO LRFD, 2014; JTG/T D64-01-2015).

However, according to the aforementioned research works, most have focused on the shear strength of headed stud, and only a few efforts have been made on investigating the deformation behavior (stiffness) of the stud, especially for headed studs using high strength steel and embedded in above mentioned new types of concrete. Shear stiffness of the headed stud connection affects the distribution of the shear flow of the studs in composite structures and hence indirectly affects the strength and fatigue life of the structures (Oehlers and Bradford 1999). Meanwhile, researchers have recognized that it is necessary to utilize accurate constitutive model (i.e., the relation between shear load and slip) of headed stud for analyzing the structural behavior of composite constructions in the whole service life by nonlinear finite element simulation or theoretical calculation (Ranzi *et al.* 2013, Spacone and El-Tawil 2004). Therefore, more attentions on the stiffness and ductility of headed studs are thought to be required. Theoretical equation that is easy to assess the shear stiffness of headed studs should be developed for design applications.

This study firstly reviewed totally 206 monotonic push-out tests from the literature to investigate the shear stiffness of headed studs embedded in various types of concrete (NC, HPC, UHPC etc.). The definition and prediction of shear stiffness for headed studs with a diameter ranging from 10 to 30 mm in various types of concrete with compressive strength ranging from 22.0 to 200.0 MPa was proposed and compared with push-out test results. Then, the effects of shear stiffness on the elastic behaviors of composite girders with different sizes and under different loading conditions were analyzed, the equations for calculating the stress and deformation of simply supported composite girders considering the influence of connection's shear stiffness were derived under different loading conditions using classical linear partial-interaction theory. Finally, the connector's shear stiffness was recommended for fully connection in composite girders with different dimensions

under different loading conditions. The findings from present study may provide a reference for the prediction of shear stiffness for headed studs and the elastic design of steel-concrete composite girder.

2. Shear stiffness definition and prediction

2.1 Shear mechanism of headed studs

Generally, the shear behaviors of headed studs are investigated through standard push-out tests. According to the observed failure modes and deformation properties (Lin *et al.* 2016, Xu *et al.* 2014, Xu and Liu 2016, 2019), the shear mechanism of the headed stud can be obtained and is described in Fig. 1, the stud is subjected to the combination of bending moment (M), axial force (N), and shear force (V) at the welding root at the same time in the push-out tests. The applied load (P) is transferred to the shear force (V) of stud and in equilibrium with the reaction forces from concrete (q_{con}). Due to the splitting tendency of concrete slab from the steel section, an axial force (N) at the root of headed stud is induced and resisted by the friction force along the stud and the reaction at the head of the stud. At the same time, the studs bend near the root, and moments (M) at the root and head of the stud are induced to satisfy rotation equilibrium.

2.2 Shear stiffness definition

Typically, the shear behaviors of headed studs in push-out test are expressed by the load-slip curves, which can be divided into three stages, as shown in Fig. 2: Stage I, the load increases linearly with the slip at initial loading stage (load generally less than 0.2~0.5 times of ultimate load). Then, in Stage II, the slope of the load-slip curve decreases with gradual deterioration of concrete due to cracking or crushing. Finally, the specimens fail after a rapid increase in slip due to the yield of the stud or the fracture of the concrete in Stage III.

The first deformation stage can be characterized by shear stiffness (k_s) which is defined as the secant stiffness of the load-slip curve at a certain load (V_e) or slip (s_e).

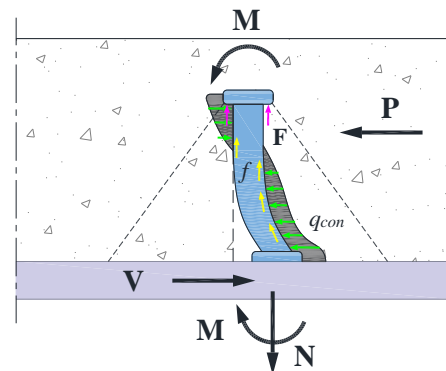


Fig. 1 Shear transfer mechanism in push-out test

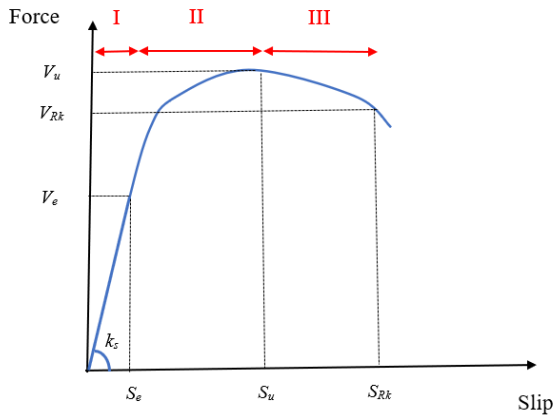


Fig. 2 Typical load-slip curve for studs in push-out test

At this stage, concrete and steel can be taken as elastic material. However, there is no unified definition of the shear connector stiffness. Till now, based on the experimental data of push-out tests, several equations for shear stiffness of headed stud in normal strength concrete (NC) were proposed. Johnson and May (1975) defined the shear stiffness of stud as the secant stiffness at $0.5 V_u$. Wang (1998) conservatively calculated the stiffness of a shear connector by assuming that at design strength ($0.8 V_u$), the shear connector has an equivalent slip of 0.8 mm. Eurocode 4 (CEN 2005) suggests the stiffness to be taken as the secant stiffness at $0.7 V_{Rk}$, in which V_{Rk} is the characteristic resistance of the shear connector ($V_{Rk}=0.9 V_u$). Alternatively, an approximate value of 100 kN/mm was assumed for headed stud with diameter of 19 mm. JSCE (2009) uses the secant stiffness at ($V_u/3$) as the shear stiffness. Based on relation between slip and head stud's diameter provided by Oehlers and Coughlan (1986), Shim *et al.* (2004) gave the equation of shear stiffness as the following equation

$$k_s = \frac{0.5 V_u}{s_{0.5 V_u}} = \frac{V_u}{(0.16 - 0.0017 f_{cu}) \cdot D_s} \quad (1)$$

where, D_s is the stud diameter (mm); and f_{cu} is the cubic compressive strength of concrete (MPa). The value of 0.16 can be substituted by 0.08 and 0.24 for the upper and lower characteristic stiffness, respectively.

However, it was reported by Shim *et al.* (2004) that for studs with diameter larger than or equal to 25 mm, the measured values from Eq. (1) were about two times larger than the calculated ones, indicating that the formula is much conservative. Meanwhile, the formula cannot predict the shear stiffness of studs in high-strength concrete or UHPC because the denominator in this equation, $(0.16 - 0.0017 f_{cu})$, would be zero or negative if the concrete strength is larger than 94.1 MPa. Meanwhile, the influence of E_c was not considered in this formula. Hence, it would fail to explain why studs have different stiffness in concrete with different E_c when the concrete strengths are the same, such as crumb rubber concrete (Han *et al.* 2015). Through the above analysis, it can be concluded that the application of Eq. (1) is limited.

Except for the definition of shear stiffness at a certain load, Lin *et al.* (2016) defined shear stiffness as the secant slope of shear load-slip curve at the slip of 0.2 mm, while the shear force at the slip of 0.2 mm is about 40% of the ultimate shear force.

In order to understand the relation of shear force at the slip of 0.2 mm ($V_{s0.2}$) and the ultimate shear force (V_u) for different types of concrete (such as normal strength concrete-NC; Light weight concrete-LWC; crumb rubber concrete-CRC; engineered cementitious composite concrete-ECC; high performance concrete or ultra-high performance concrete-HPC/UHPC) with different compressive strength, totally 206 monotonic push-out test specimens were reviewed (Viest 1956, Davies 1967, Ollgaard *et al.* 1971, Shim *et al.* 2004, Xue *et al.* 2008, Valente and Cruz 2009, Wang 2013, Han *et al.* 2015, Kim *et al.* 2015, Luo *et al.* 2016, Tian and Du 2016, Lin 2016, Zhan *et al.* 2020, Qi *et al.* 2019, Wang *et al.* 2018, 2019, Xu *et al.* 2018, Liu *et al.* 2018, Dominic *et al.* 2018). Fig. 3 shows the relation of $V_{s0.2}/V_u$ and concrete strength for shear stud in various types of concrete. For concrete strength less than 80 MPa, most of $V_{s0.2}/V_u$ change from 0.2 to 0.6, no obvious trend for the change of $V_{s0.2}/V_u$ with concrete strength, so the frequency distribution of $V_{s0.2}/V_u$ for studs in concrete whose compressive strength is less than 80 MPa is plotted in Fig. 4, and it meets a normal distribution with mean of 0.39 and standard deviation of 0.1. As for the studs in high strength concrete (>80 MPa), the value of $V_{s0.2}/V_u$ increase with concrete strength, and most of the value is larger than 0.5, indicating that the stud is no longer in elastic state when slip at 0.2 mm, therefore, it is questionable still define elastic shear stiffness as the secant slope of shear load-slip curve at the slip of 0.2 mm.

Therefore, in this study the shear stiffness of studs is defined as the secant stiffness of the load-slip curve at $0.5 V_u$, because it can not only consists with the definition at slip of 0.2 mm for concrete strength less than 80 MPa, but also keeps the stud embedded in high strength concrete (>80 MPa) still within elastic state.

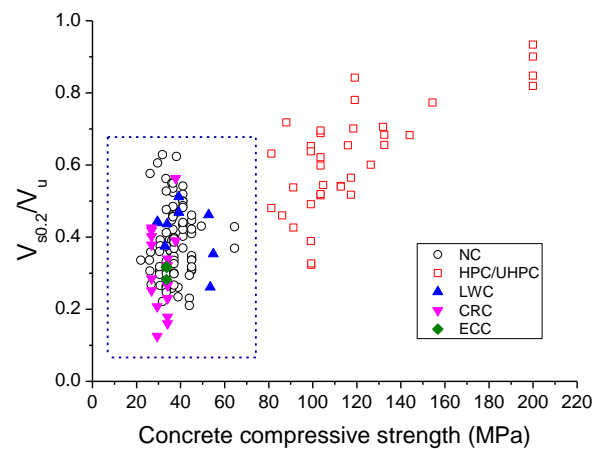


Fig. 3 The relation of $V_{s0.2}/V_u$ and concrete strength for shear stud in various types of concrete

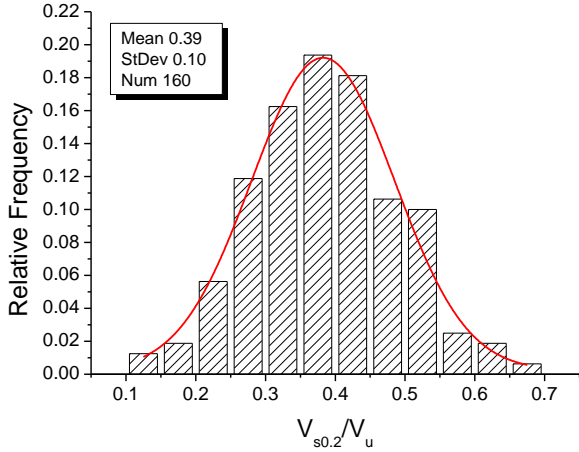


Fig. 4 The frequency distribution of $V_{s0.2}/V_u$ for studs in concrete ($f_c < 80$ MPa)

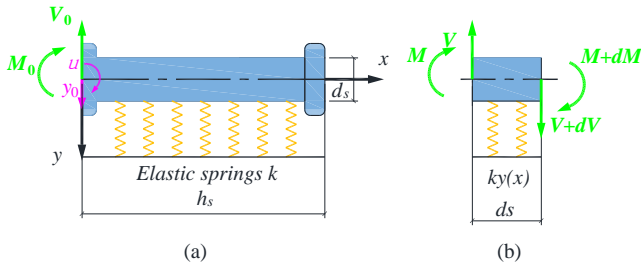


Fig. 5 Analytical model of stud in concrete: (a) stud on an elastic foundation and (b) differential element of length dx

3. Analytical model for predicting shear stiffness

Based on the shear mechanism of headed stud as shown in Fig. 1 (Lin *et al.* 2016, Xu and Liu 2016, 2019), the structural behavior of headed studs embedded in concrete under shear loading can be analogous to a beam on an elastic foundation, which supported by a series of continuous elastic springs.

Fig. 5 shows an analytical model of headed stud under combined shear force V and bending moment M at the root of shank, in which, the diameter and height of stud is d_s and h_s respectively; the elastic modulus and the inertia of moment of the steel stud is E_s and I_s , respectively; $y(x)$ is the deflection of stud at the position x from the root.

3.1 Basic assumption

In order to simplify the theoretical derivation of the shear stiffness of headed stud, the following assumptions are made:

- (1) The flexural deformation of the stud conforms to the plane section assumption.
- (2) Perfect contact between the stud and concrete is assumed during the loading process.
- (3) Both steel and concrete are in elastic range.
- (4) The axial force of stud and friction force at interface are ignored.

3.2 Differential equation

Fig. 5(b) shows the equilibrium state of force for infinitesimal element (dx) from the beam on elastic foundation, the shear force V , $V+dV$, and the bending moment M , $M+dM$ are act on two ends, and reaction distribution stress σ is at the bottom.

According to the equilibrium of force and moment, the following equations can be obtained:

$$\sigma = \frac{dV}{dx}; \quad V = \frac{dM}{dx} \quad (2)$$

So, the relation between σ and M is expressed:

$$\sigma = \frac{d^2 M}{dx^2} \quad (3)$$

Based on the assumptions (1) and (3), the bending moment is proportional to the curvature θ :

$$\theta = \frac{dy}{dx} \quad (4)$$

$$M = -\frac{1}{E_s I_s} \frac{d^2 y}{dx^2} \quad (5)$$

$$V = -\frac{1}{E_s I_s} \frac{d^3 y}{dx^3} \quad (6)$$

Based on Winkler's hypothesis, the reaction force $\sigma(x)$ is proportional to the deformation y of beam on elastic foundation.

$$\sigma = ky d_s \quad (7)$$

where k is stiffness, which is determined as the resistance of concrete per area when unit deflection is applied to stud, $k = CE_c/d_s$. C is a constant related to the properties of concrete, and E_c is the elastic modulus of concrete.

Therefore, deflection differential equation of beam on elastic foundation can be obtained from the above equations

$$\frac{d^4 y}{dx^4} + \frac{kd_s}{E_s I_s} y = 0 \quad (8)$$

Define the flexibility coefficient $\alpha = \sqrt[4]{kd_s/(4E_s I_s)}$, the general solution of the above Eq. (8) is

$$y = e^{\alpha x} (A_1 \cos \alpha x + A_2 \sin \alpha x) + e^{-\alpha x} (A_3 \cos \alpha x + A_4 \sin \alpha x) \quad (9)$$

Considering the boundary condition at both ends:

$$\begin{cases} y|_{x=0} = y_0; \theta|_{x=0} = \theta_0 \\ M|_{x=0} = M_0; V|_{x=0} = V_0 \end{cases} \quad (10)$$

The deformation and forces can be expressed as follows

$$\begin{cases} y = y_0\varphi_1 + \theta_0 \frac{1}{2\alpha} \varphi_2 - M_0 \frac{2\alpha^2}{k} \varphi_3 - V_0 \frac{\alpha}{k} \varphi_4 \\ \theta = -y_0\alpha\varphi_4 + \theta_0\varphi_1 - M_0 \frac{2\alpha^3}{k} \varphi_2 - V_0 \frac{2\alpha^2}{k} \varphi_3 \\ M = y_0 \frac{k}{2\alpha^2} \varphi_3 + \theta_0 \frac{k}{4\alpha^3} \varphi_4 + M_0\varphi_1 + V_0 \frac{1}{2\alpha} \varphi_2 \\ V = y_0 \frac{k}{2\alpha} \varphi_2 + \theta_0 \frac{k}{2\alpha^2} \varphi_3 - M_0\alpha\varphi_4 + V_0\varphi_1 \end{cases} \quad (11)$$

where

$$\begin{cases} \varphi_1 = ch\alpha x \cos \alpha x \\ \varphi_2 = ch\alpha x \sin \alpha x + sh\alpha x \cos \alpha x \\ \varphi_3 = sh\alpha x \sin \alpha x \\ \varphi_4 = ch\alpha x \sin \alpha x - sh\alpha x \cos \alpha x \end{cases} \quad (12)$$

3.3 Solution

Since the deformation and bending moment at the free end of stud ($x=h_s$) is 0, then

$$\begin{cases} y|_{x=h_s} = 0 \\ M|_{x=h_s} = 0 \end{cases} \quad (13)$$

Substituting Eq. (13) into Eq. (11), get:

$$\begin{cases} y_0 = \frac{M_0}{2E_s I_s \alpha^2} n_1 + \frac{V_0}{4E_s I_s \alpha^3} n_2 \\ \theta_0 = \frac{M_0}{E_s I_s \alpha} n_3 + \frac{V_0}{2E_s I_s \alpha^2} n_4 \end{cases} \quad (14)$$

where

$$\begin{cases} n_1 = \frac{\varphi_1\varphi_2 + \varphi_3\varphi_4}{\varphi_1\varphi_4 - \varphi_2\varphi_3} \\ n_2 = \frac{\varphi_2^2 + \varphi_4^2}{\varphi_1\varphi_4 - \varphi_2\varphi_3} \\ n_3 = \frac{\varphi_1^2 + \varphi_3^2}{\varphi_2\varphi_3 - \varphi_1\varphi_4} \\ n_4 = \frac{\varphi_1\varphi_2 + \varphi_3\varphi_4}{\varphi_2\varphi_3 - \varphi_1\varphi_4} \end{cases} \quad (15)$$

When the unit shear force acts on the fix end of stud:

$$\begin{cases} y|_{x=0} = \delta_{VV}; \theta|_{x=0} = -\delta_{VM} \\ M|_{x=0} = 0; V|_{x=0} = 1 \end{cases} \quad (16)$$

When the unit moment acts on the fix end of stud:

$$\begin{cases} y|_{x=0} = \delta_{MV}; \theta|_{x=0} = -\delta_{MM} \\ M|_{x=0} = 1; V|_{x=0} = 0 \end{cases} \quad (17)$$

Combining the above equations (14,16,17), the solutions are

$$\begin{cases} \delta_{VV} = \frac{n_2}{4E_s I_s \alpha^3} \\ \delta_{MV} = \frac{n_1}{2E_s I_s \alpha^3} \\ \delta_{VM} = -\frac{n_4}{2E_s I_s \alpha^2} \\ \delta_{MM} = -\frac{n_3}{E_s I_s \alpha^2} \end{cases} \quad (18)$$

Therefore, when both shear force (V) and bending moment (M) act on the fixed end, the deformation is:

$$\begin{cases} y_0 = V\delta_{VV} + M\delta_{MV} \\ \theta_0 = -(V\delta_{VM} + M\delta_{MM}) \end{cases} \quad (19)$$

Generally, there is no rotation at fixed end of stud, i.e., $\theta_0=0$

$$y_0 = V\delta_{VV} + M\delta_{MV} = \frac{V}{4E_s I_s \alpha^3} (n_2 - \frac{n_1 n_4}{n_3}) \quad (20)$$

Eq. (20) can be recognized as

$$V = 4E_s I_s \alpha^3 \frac{1}{(n_2 - \frac{n_1 n_4}{n_3})} y_0 \quad (21)$$

When $ah_s \geq 4.5$ 时, the value of n_i ($i=1,2,3,4$) converge to a constant, so

$$V = 0.267 d_s c^{\frac{3}{4}} E_c^{\frac{3}{4}} E_s^{\frac{1}{4}} y_0 \quad (22)$$

Thus, the shear stiffness can be determined as

$$k_s = 0.267 d_s c^{\frac{3}{4}} E_c^{\frac{3}{4}} E_s^{\frac{1}{4}} = C d_s E_c^{\frac{3}{4}} E_s^{\frac{1}{4}} \quad (23)$$

where, k_s is the shear stiffness, kN/mm; E_s is the elastic module of steel plate, MPa; E_c is the elastic module of concrete, MPa; d_s is the diameter of stud, mm.

Eq. (23) shows that the main factors affecting the shear stiffness are the elastic modulus of concrete, the elastic modulus of the stud, the diameter of stud, which are in good agreement with test and FEA results (Wang 2013, Lin 2016).

The parameter C is a constant related to the properties of concrete. The value of parameter C can be fitted by the test and FEA data. A total of 169 push-out tests data for studs in normal-strength concrete (<80 MPa) and 37 tests in HPC/UHPC (>80 MPa) were used for a linear regression analysis to get the value of C, as shown in Fig.6. The value of C is fitted as 0.374 for studs in NC and HPC/UHPC. The value of C for studs in present study is slightly larger than that (0.32) proposed previously by Lin (2016), because the equation of shear stiffness of headed stud proposed by Lin

(2016) did not include the studs embedded in HPC/UHPC. Fig. 7 shows the comparison of shear stiffness from prediction using Eq. (23) and that from push-out tests. The mean ratio of predicted shear stiffness to test ones is 1.03 for studs in NC and HPC/UHPC, with the standard deviation of 0.17, indicating that the shear stiffness of headed studs in NC and HPC/UHPC can be predicted accurately by Eq. (23) using parameter C of 0.374.

4. Effect of shear stiffness of connectors on structural behavior of composite girder

To understand the effect of the connector’s shear stiffness on the mechanical behavior of steel-concrete composite girder at serviceability limit state, the deflection and cross-sectional stress considering the influence of connection’s shear stiffness under different loading were derived theoretically and evaluated accordingly (Johnson 2008).

4.1 Geometric models and basic assumptions

A simply supported girder with equal cross-section was selected to study the effect of connection’s shear stiffness on the elastic behavior of steel-concrete composite girder at serviceability limit state, as shown in Fig. 8. The total span is L , the concrete slab with width of w_c and thickness of t_c is connected to steel I-girder (in which f_w, f_t is the width and thickness of flange; w_h, w_t is the height and thickness of the web, respectively) with the help of shear connectors, such as headed studs. E_c and A_c is the modulus of elasticity and area of concrete deck; I_c is the moment of inertia with respect to its own centroid. Similarly, E_s, A_s and I_s are the modulus of elasticity, area and the moment of inertia of steel girder. The intersection points of the cross-sectional symmetry axis (central line) with the top and bottom of concrete deck are defined as point 1 and 2, and the intersection points with the top and bottom of steel girder are defined as point 3 and 4.

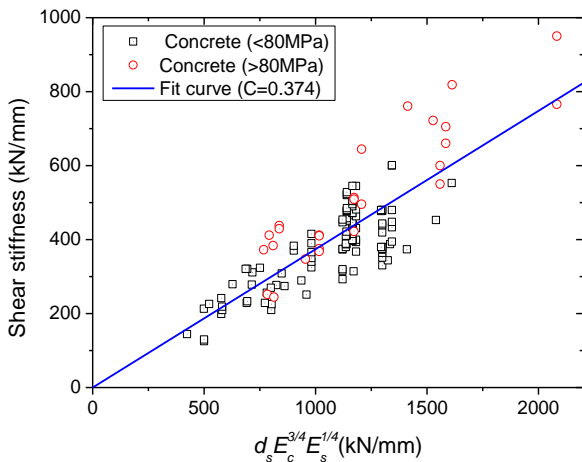


Fig. 6 Fitting of shear stiffness

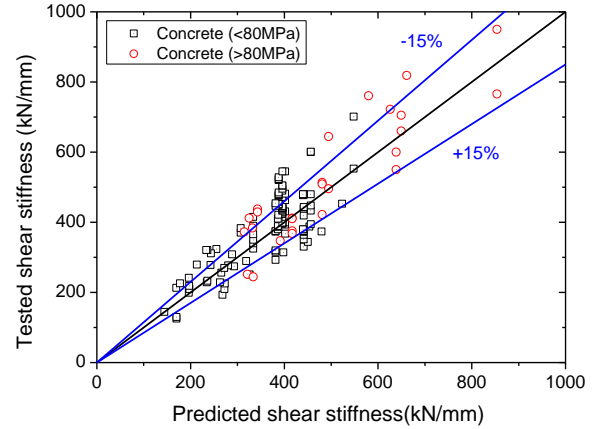


Fig. 7 Comparison between predicted and tested shear stiffness

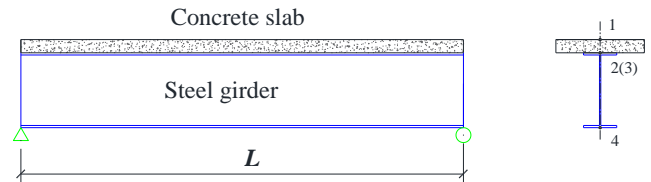


Fig. 8 Simply supported steel-concrete girder

The y_{c1} and y_{c2} are the distances from point 1 and 2 to the centroid of the concrete deck, respectively; while y_{s3} and y_{s4} are the distances from point 3 and 4 to the centroid of steel girder, respectively. The total number of weld shear studs at steel-concrete interface is n_s , and the shear stiffness of one stud is k_s , which can be predicted by Eq. (23), then the shear stiffness per unit length at the interface is

$$K_s = n_s k_s / L \tag{24}$$

The following basic assumptions are made during the theoretical derivation:

- (1) The material is in elastic stage.
- (2) Concrete slab and steel girder satisfy the assumption of plane section, respectively.
- (3) The curvature of concrete deck and steel beam is consistent.

The structural behaviors of steel-concrete composite girder were analyzed when subjected to different loading, such as uniformly distributed loading, concentrated loading, and temperature difference. The details of theoretical derivation for composite girder under uniformly distributed loading were described in the following. But, only the derivation results under other loading condition were listed due to the limited space.

4.2 Structural behavior of composite girder under uniformly distributed loading

It is assumed that the top surface of composite girder is subjected to a uniformly distributed load p . As shown in Fig. 9, the segment with the length of x (from support O) is

selected as the research object. The shear flow is assumed to be $q(x)$ per unit length at steel-concrete interface. At section A , the axial force $N_c(x)$, $N_s(x)$ and bending moment $M_c(x)$, $M_s(x)$ are applied to the concrete slab and steel girder, respectively.

At section A , from the equilibration of axial force and bending moment, the following equations can be obtained

$$N_c(x) - N_s(x) = 0 \quad (25)$$

$$M_c(x) + M_s(x) + N_c(x)h_0 = pLx/2 - px^2/2 \quad (26)$$

Since the concrete slab and the steel beam have the same curvature after deformation, then

$$\frac{M_c(x)}{E_c I_c} = \frac{M_s(x)}{E_s I_s} \quad (27)$$

From the equilibration of axial force (in longitude direction) of concrete slab

$$N_c(x) = \int_0^x q(t)dt \quad (28)$$

Under the applied load p , relative slip between point 2 and 3 at steel-concrete interface may occur, resulting in the assumption of plane section for the composite section invalid. And the difference between these two points ($\varepsilon_2 - \varepsilon_3$) is defined as the slip strain $\varepsilon_{\text{slip}}$

$$\varepsilon_{\text{slip}}(x) = \frac{ds(x)}{dx} = \varepsilon_2(x) - \varepsilon_3(x) \quad (29)$$

In addition, the shear flow $q(x)$ per unit length on the steel-concrete interface is the product of the shear stiffness per unit and the relative slip at the corresponding position

$$q(x) = K_s s(x) \quad (30)$$

The right term of Eq. (29) is calculated as

$$\begin{aligned} \varepsilon_{\text{slip}} &= \varepsilon_2 - \varepsilon_3 = \frac{N_c}{E_c A_c} + \frac{N_s}{E_s A_s} - \frac{M_c y_{c2}}{E_c I_c} - \frac{M_s y_{s3}}{E_s I_s} \\ &= N_c \left(\frac{1}{E_c A_c} + \frac{1}{E_s A_s} + \frac{h_0^2}{EI} \right) - \frac{h_0 p (Lx - x^2)}{2EI} \end{aligned} \quad (31)$$

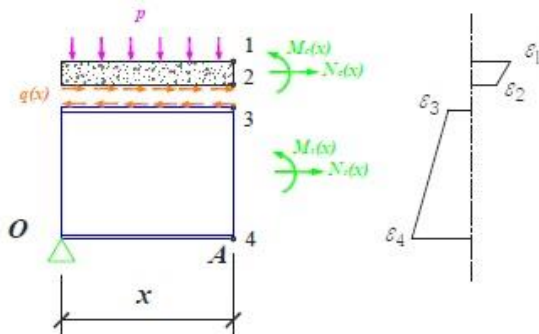


Fig. 9 Internal force and strain state for segment x under uniformly distributed load

where, h_0 is the distance between the centroid of concrete slab and steel beam, i.e., $h_0 = y_{c2} + y_{s3}$; EI is the sum of moment of inertia for concrete slab and steel beam, $EI = E_c I_c + E_s I_s$.

The left term of Eq. (29) is calculated as

$$\varepsilon_{\text{slip}} = \frac{ds(x)}{dx} = \frac{d^2 N_c(x)}{K_s dx^2} \quad (32)$$

Combining Eq.(31) and Eq. (32), get

$$N_c''(x) - \lambda^2 N_c(x) = -\frac{h_0 p (Lx - x^2) K_s}{2EI} \quad (33)$$

where $\lambda^2 = K_s \delta$; $\delta = \left(\frac{1}{E_c A_c} + \frac{1}{E_s A_s} + \frac{h_0^2}{EI} \right)$

Eq. (33) is a second-order linear differential equation with constant coefficients, its general solution is

$$\begin{aligned} N_c(x) &= C_1 \sinh(\lambda x) + C_2 \cosh(\lambda x) \\ &\quad + \frac{h_0 p K_s (Lx - x^2 - 2/\lambda^2)}{2\lambda^2 EI} \end{aligned} \quad (34)$$

According to the boundary conditions: $x=0$, $N_c(0)=0$, and $s(L/2)=0$, the coefficients C_1 and C_2 can be obtained

$$C_1 = \frac{h_0 p K_s \tanh(\lambda L/2)}{\lambda^4 EI}; \quad C_2 = \frac{h_0 p K_s}{\lambda^4 EI} \quad (35)$$

Therefore

$$N_c(x) = \frac{h_0 p K_s}{2\lambda^2 EI} \left[-\frac{2}{\lambda^2} \tanh\left(\frac{\lambda L}{2}\right) \sinh(\lambda x) + \frac{2}{\lambda^2} \cosh(\lambda x) + \left(Lx - x^2 - \frac{2}{\lambda^2} \right) \right] \quad (36)$$

$$q(x) = \frac{h_0 p K_s}{2\lambda^2 EI} \left[-\frac{2}{\lambda} \tanh\left(\frac{\lambda L}{2}\right) \cosh(\lambda x) + \frac{2}{\lambda} \sinh(\lambda x) + (L - 2x) \right] \quad (37)$$

$$s(x) = \frac{h_0 p}{2\lambda^2 EI} \left[-\frac{2}{\lambda} \tanh\left(\frac{\lambda L}{2}\right) \cosh(\lambda x) + \frac{2}{\lambda} \sinh(\lambda x) + (L - 2x) \right] \quad (38)$$

$$\varepsilon_{\text{slip}}(x) = \frac{h_0 p}{2\lambda^2 EI} \left[-2 \tanh\left(\frac{\lambda L}{2}\right) \sinh(\lambda x) + 2 \cosh(\lambda x) - 2 \right] \quad (39)$$

Based on the elementary beam theory, the stress at points 1, 2, 3 and 4 are calculated as follows

$$\begin{aligned}\sigma_{c1} &= \frac{N_c}{A_c} + \frac{M_c y_{c1}}{I_c} \\ &= \frac{N_c}{A_c} + \frac{(pLx/2 - px^2/2 - N_c h_0) E_c I_c y_{c1}}{I_c EI}\end{aligned}\quad (40)$$

$$\begin{aligned}\sigma_{c2} &= \frac{N_c}{A_c} - \frac{M_c y_{c2}}{I_c} \\ &= \frac{N_c}{A_c} - \frac{(pLx/2 - px^2/2 - N_c h_0) E_c I_c y_{c2}}{I_c EI}\end{aligned}\quad (41)$$

$$\begin{aligned}\sigma_{s3} &= \frac{N_c}{A_c} - \frac{M_s y_{s3}}{I_s} \\ &= \frac{N_c}{A_c} - \frac{(pLx/2 - px^2/2 - N_c h_0) E_s I_s y_{s3}}{I_s EI}\end{aligned}\quad (42)$$

$$\begin{aligned}\sigma_{s4} &= \frac{N_c}{A_c} + \frac{M_s y_{s4}}{I_s} \\ &= \frac{N_c}{A_c} + \frac{(pLx/2 - px^2/2 - N_c h_0) E_s I_s y_{s4}}{I_s EI}\end{aligned}\quad (43)$$

The deflection can be obtained through double integral of curvature along beam length:

$$y(x) = \iint \phi(x) dx dx = \iint \frac{M_c + M_s}{EI} dx dx \quad (44)$$

$$y(x) = \frac{1}{EI} \left\{ \begin{aligned} &\left[\frac{pLx^3}{12} - \frac{px^4}{24} - \frac{h_0^2 p K_s}{2\lambda^2 EI} \left[\frac{-2}{\lambda^4} \tanh\left(\frac{\lambda L}{2}\right) \sinh(\lambda x) + \frac{2}{\lambda^4} \cosh(\lambda x) + \frac{Lx^3}{6} - \frac{x^4}{12} - \frac{x^2}{\lambda^2} \right] \right. \\ &\left. + C_3 x + C_4 \right] \end{aligned} \right\} \quad (45)$$

According to the boundary conditions: $x=0, y(0)=0$, and the rotation at middle span $y'(L/2)=0$, the coefficients C_3 and C_4 can be obtained:

$$C_3 = -\left[\frac{pL^3}{24} - \frac{h_0^2 p K_s}{2\lambda^2 EI} \left(\frac{L^3}{12} - \frac{L}{\lambda^2} \right) \right]; \quad C_4 = \frac{h_0^2 p K_s}{\lambda^6 EI} \quad (46)$$

If concrete slab and steel beam are fully connected, the strain induced by relative slip is 0, i.e., $\varepsilon_{slip}=0$, the strain at top or bottom of concrete slab and steel beam can also be calculated by Eqs. (40)-(43), the axial force $N_c(x)$ at centroid of concrete slab is:

$$N_c(x) = \frac{h_0 p (Lx - x^2)}{2\delta EI} \quad (47)$$

And the corresponding deflection can be determined as follows

$$y(x) = \frac{1}{EI} \left[\frac{pLx^3}{12} - \frac{px^4}{24} - \frac{h_0^2 p}{2\delta EI} \left(\frac{Lx^3}{6} - \frac{x^4}{12} \right) + C_5 x + C_6 \right] \quad (48)$$

$$C_5 = -\left(\frac{pL^3}{24} - \frac{h_0^2 p L^3}{24\delta EI} \right); \quad C_6 = 0$$

The theoretical derivation for composite girder under concentrated load P or temperature difference T (the difference between temperature at concrete slab and steel beam) is almost the same as that under uniform distributed load q , the stress and deflection at section x for composite girder under concentrated load P or temperature difference T are listed in Table 1, both the conditions of partial connected and “full connected” are considered for comparison.

4.3 The effect of shear stiffness under different loading conditions

In order to understand the structural behaviors of steel-concrete girder under different loading conditions, the headed studs with different diameters and shear stiffness were considered. Also, the limit value of shear stiffness for the “full connection” design was provided to guide the selection of shear connectors.

A case study was conducted for quantitatively and comparatively analysis on the effects of shear stiffness under different loading conditions including uniform distributed loading, concentrated loading and temperature difference. A simply supported steel-concrete composite girder with span (L) of 16m was selected as the research object. The width and depth of concrete slab is 2400 mm and 240 mm, respectively. The width and thickness of top flange for steel beam is 300 mm and 20 mm, while is 400 mm and 20 mm of bottom flange. The height and thickness of web is 560 mm and 12 mm. The design compressive strength of concrete slab is 22.4 MPa with elastic modulus of 3.45×10^4 MPa, while the design strength of steel web and flange is 275 MPa and 270 MPa with elastic modulus of 2.06×10^5 MPa. According to design specification JTG/T D64-01(2015) and proposed Eq. (23) for shear stiffness, the design shear strength of headed studs with diameter of 19 mm, 22 mm and 25 mm is 87.5 kN, 117.3 kN and 151.4 kN, while the shear stiffness is 348 kN/mm, 403 kN/mm and 458 kN/mm.

The elastic design method was used to design and arrange the welded studs at steel-concrete interface. The material properties of steel and concrete adopt design values. The maximum bending moment section of the composite girder reaches the elastic ultimate bending capacity when subjected to external loading was defined as elastic limit state.

According to Eqs. (49) and (50), the number of shear studs (n_s) can be determined.

Table 1 The stress and deflection at section x for composite girder

Connect condition	Item	Under concentrated load P	Under Temperature difference T
Partial connected	Stress	$\sigma_{c1} = \frac{N_c}{A_c} + \frac{M_c y_{c1}}{I_c} = \frac{N_c}{A_c} + \frac{(Px/2 - N_c h_0) E_c I_c y_{c1}}{I_c EI} \quad (P-1)$	$\sigma_{c1} = \frac{N_c}{A_c} + \frac{M_c y_{c1}}{I_c} = \frac{N_c}{A_c} - \frac{N_c h_0 E_c I_c y_{c1}}{I_c EI} \quad (T-1)$
		$\sigma_{c2} = \frac{N_c}{A_c} - \frac{M_c y_{c2}}{I_c} = \frac{N_c}{A_c} - \frac{(Px/2 - N_c h_0) E_c I_c y_{c2}}{I_c EI} \quad (P-2)$	$\sigma_{c2} = \frac{N_c}{A_c} - \frac{M_c y_{c2}}{I_c} = \frac{N_c}{A_c} + \frac{N_c h_0 E_c I_c y_{c2}}{I_c EI} \quad (T-2)$
		$\sigma_{s3} = \frac{N_c}{A_c} - \frac{M_s y_{s3}}{I_s} = \frac{N_c}{A_c} - \frac{(Px/2 - N_c h_0) E_s I_s y_{s3}}{I_s EI} \quad (P-3)$	$\sigma_{s3} = \frac{N_c}{A_c} - \frac{M_s y_{s3}}{I_s} = \frac{N_c}{A_c} + \frac{N_c h_0 E_s I_s y_{s3}}{I_s EI} \quad (T-3)$
		$\sigma_{s4} = \frac{N_c}{A_c} + \frac{M_s y_{s4}}{I_s} = \frac{N_c}{A_c} + \frac{(Px/2 - N_c h_0) E_s I_s y_{s4}}{I_s EI} \quad (P-4)$	$\sigma_{s4} = \frac{N_c}{A_c} + \frac{M_s y_{s4}}{I_s} = \frac{N_c}{A_c} - \frac{N_c h_0 E_s I_s y_{s4}}{I_s EI} \quad (T-4)$
		$N_c = \frac{Ph_0 K_s}{2\lambda^3 EI} \left[\lambda x - \frac{\sinh(\lambda x)}{\cosh(\lambda L/2)} \right] \quad (P-5)$	$N_c(x) = \frac{\alpha_T \Delta T K_s}{\lambda^2} \left[\tanh\left(\frac{\lambda L}{2}\right) \sinh(\lambda x) - \cosh(\lambda x) + 1 \right] \quad (T-5)$
Full connected	Deflection	$y(x) = \frac{1}{EI} \left\{ \frac{Px^3}{12} - \frac{h_0^2 PK_s}{2\lambda^3 EI} \left[\frac{\lambda x^3}{6} - \frac{\sinh(\lambda x)}{\lambda^2 \cosh(\lambda L/2)} \right] + C_3 x + C_4 \right\}$ $C_3 = -\left[\frac{PL^3}{16} - \frac{h_0^2 PK_s}{2\lambda^3 EI} \left(\frac{\lambda L^2}{8} - \frac{1}{\lambda} \right) \right]; \quad C_4 = 0 \quad (P-6)$	$y(x) = \frac{\alpha_T \Delta T K_s h_0}{\lambda^2 EI} \left[\frac{1}{\lambda^2} \tanh\left(\frac{\lambda L}{2}\right) \sinh(\lambda x) - \frac{\cosh(\lambda x)}{\lambda^2} + \frac{x^2}{2} + C_5 x + C_6 \right];$ $C_5 = -\frac{L}{2}; \quad C_6 = \frac{1}{\lambda^2} \quad (T-6)$
	Stress	$N_c = \frac{Ph_0 x}{2\delta EI} \quad (P-7)$ <p>(P-1) ~ (P-4)</p>	$\sigma_{c1} = \frac{N_c}{A_c} + \frac{M_c y_{c1}}{I_c} = \frac{\alpha_T \Delta T}{\delta} \left(\frac{1}{A_c} - \frac{h_0 E_c y_{c1}}{EI} \right) \quad (T-7)$ $\sigma_{c2} = \frac{N_c}{A_c} - \frac{M_c y_{c2}}{I_c} = \frac{\alpha_T \Delta T}{\delta} \left(\frac{1}{A_c} + \frac{h_0 E_c y_{c2}}{EI} \right) \quad (T-8)$ $\sigma_{s3} = \frac{N_c}{A_c} - \frac{M_s y_{s3}}{I_s} = \frac{\alpha_T \Delta T}{\delta} \left(\frac{1}{A_c} + \frac{h_0 E_s y_{s3}}{EI} \right) \quad (T-9)$ $\sigma_{s4} = \frac{N_c}{A_c} + \frac{M_s y_{s4}}{I_s} = \frac{\alpha_T \Delta T}{\delta} \left(\frac{1}{A_c} - \frac{h_0 E_s y_{s4}}{EI} \right) \quad (T-10)$
	Deflection	$y(x) = \frac{1}{EI} \left(\frac{Px^3}{12} - \frac{Ph_0^2 x^3}{12\delta EI} + C_5 x + C_6 \right);$ $C_5 = -\left(\frac{PL^3}{16} - \frac{h_0^2 PL^2}{16\delta EI} \right); \quad C_6 = 0 \quad (P-8)$	$y(x) = \frac{\alpha_T \Delta T h_0}{\delta EI} \left(\frac{x^2}{2} - \frac{Lx}{2} \right) \quad (T-11)$

$$q(x) = \frac{V(x)S_c}{I_{eq}} \quad (49)$$

$$n_s = \frac{ql}{V_d} \quad (50)$$

where, $q(x)$ is shear flow per unit length on the steel-concrete interface, $V(x)$ is the shear force at section x , S_c is the first moment of conversion cross-section to the elastic neutral axis; I_{eq} is the second moment of conversion section, l is the length of calculation area, V_d is the design shear strength of a stud.

When headed studs with diameter of 16 mm, 19 mm, 22 mm and 25 mm are used respectively, a total of 115, 82, 61 and 47 studs need to be arranged at the steel-concrete interface under concentrated load. Generally, two studs are installed in transversal direction at cross section, thus the equally spacing in longitude direction is 275 mm, 390 mm, 516 mm and 666 mm for headed studs with diameter of 16 mm, 19 mm, 22 mm and 25 mm, respectively. Under the

action of concentrated load or uniform distributed load, the maximum bending moment appear at mid-span section. When the mid-span section reaches the elastic ultimate bending capacity, the total shear flow at interface under concentrated load is the same as that under uniform distributed load. Therefore, the total number and the arrangement of studs under uniform distributed load equal to that under concentrated load when using the same diameter of studs. For the sake of contrast, the arrangement of studs under temperature difference is chosen the same. When 19 mm-studs were used, the shear stiffness per unit length ($K_{s,19}$) at the interface is 1.38×10^6 kN/m².

In the analysis, 19mm-studs were used and $K_{s,19}$ is taken as the benchmark to analyze the impact of shear stiffness at steel-concrete interface, and the shear stiffness corresponding to the arrangement of 16 mm, 22 mm and 25 mm studs is $K_{s,16} = 1.188 K_{s,19}$, $K_{s,22} = 0.864 K_{s,19}$ and $K_{s,25} = 0.760 K_{s,19}$, respectively.

4.3.1 Under uniform distributed loading

The applied uniform distributed loading is assumed to be 10 kN/m. Fig. 10 and Table 2 show the effects of shear

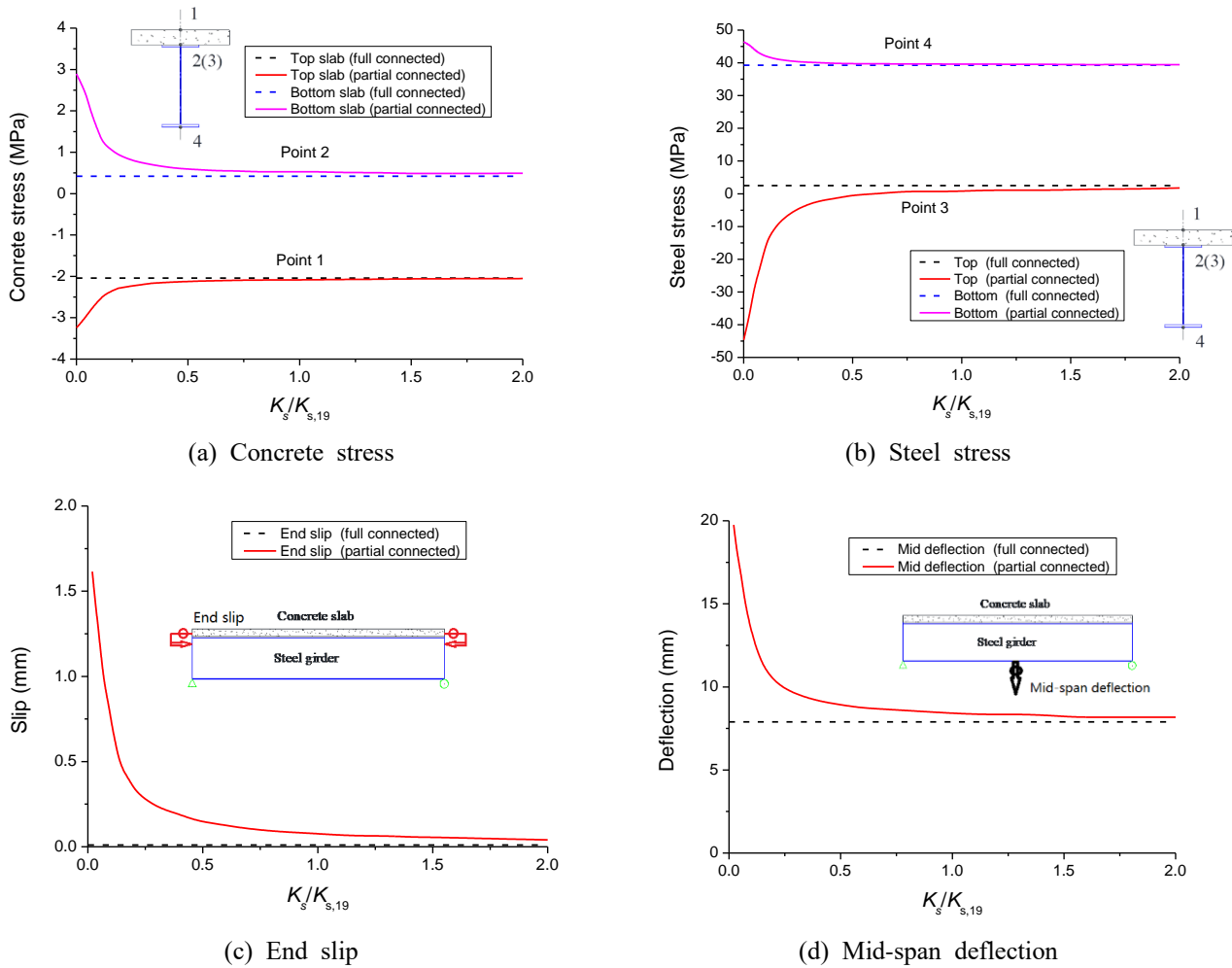


Fig. 10 Effect of shear stiffness under uniform distributed loading

stiffness on the normal stress on top (σ_{c1}) and bottom (σ_{c2}) surface of concrete slab, normal stress on top (σ_{s3}) and bottom (σ_{s4}) surface of steel beam, deflection at middle span ($y_{L/2}$), and relative slip at end section. The stress in negative indicates compression while tension in positive. When the shear stiffness is small, the effects on the stress, deflection and slip is significant, as the increasing of shear stiffness, the effects reduce gradually, and the stress, deflection and slip at partial connected condition tend to be those at full connected condition.

As the increasing of stud diameter, the shear stiffness at corresponding arrangement of studs decrease gradually, and the differences of stress and deflection between partially connection and fully connection become larger. For example, when installation of 19mm-studs, the difference of σ_{c1} , σ_{c2} , σ_{s3} , v_{s4} and $y_{L/2}$ between partially connection and fully connection is 2.2%, 21.9%, 70.8%, 0.7% and 6.5%, respectively. The difference of stress at steel-concrete interface is obvious. It should be noted that although the difference of stress σ_{s3} is large, the stress level is very low, which can be ignored in compression with the yield stress of steel. Although the value of stress σ_{c2} is small, but is in tensile for concrete, which should be pay more attention.

The difference of stress σ_{c1} , σ_{s4} is less than 5%, which can be ignored.

Under uniform distributed loading, in order to limit the difference of stress between partially connection and fully connection less than 5%, the shear stiffness should be more than 0.56×10^6 kN/m²; while to limit the difference of deflection less than 5%, the value should be more than 1.69×10^6 kN/m².

4.3.2 Under concentrated loading

The applied concentrated loading at mid-span is assumed to be 100 kN. Fig. 11 and Table 3 show the effects of shear stiffness on the normal stress on top (σ_{c1}) and bottom (σ_{c2}) surface of concrete slab, normal stress on top (σ_{s3}) and bottom (σ_{s4}) surface of steel beam, deflection at middle span ($y_{L/2}$), and relative slip at end section. Similar to that under uniform distributed loading, when the shear stiffness is small, the effects on the stress, deflection and slip is significant, as the increasing of shear stiffness, the effects reduce gradually, and the stress, deflection and slip at partial connected condition tend to be those at full connected condition, but the speed approaches to the situation at full connected condition under concentrated loading is lower than that under uniform distributed loading.

Table 2 Structural response under uniform distributed loading

Item	Partially connection-stud diameter				Fully connection	Partially connection/ Fully connection			
	16 mm	19 mm	22 mm	25 mm		16 mm	19 mm	22 mm	25 mm
σ_{c1} (MPa)	-2.081	-2.088	-2.095	-2.102	-2.044	1.018	1.022	1.025	1.029
σ_{c2} (MPa)	0.496	0.510	0.525	0.539	0.418	1.185	1.219	1.254	1.288
σ_{s3} (MPa)	1.009	0.729	0.451	0.172	2.499	0.404	0.292	0.181	0.069
σ_{s4} (MPa)	39.479	39.521	39.562	39.604	39.256	1.006	1.007	1.008	1.009
ν_{L2} (mm)	8.363	8.442	8.520	8.597	7.930	1.055	1.065	1.074	1.084

Table 3 Structural response under concentrated loading

Item	Partially connection-stud diameter				Fully connection	Partially connection/ Fully connection			
	16 mm	19 mm	22 mm	25 mm		16 mm	19 mm	22 mm	25 mm
σ_{c1} (MPa)	-2.766	-2.785	-2.803	-2.819	-2.555	1.083	1.090	1.097	1.104
σ_{c2} (MPa)	0.960	0.999	1.035	1.069	0.523	1.834	1.909	1.978	2.043
σ_{s3} (MPa)	-5.291	-6.048	-6.743	-7.397	3.124	-2.694	-2.936	-3.159	-3.368
σ_{s4} (MPa)	50.329	50.442	50.546	50.644	49.070	1.026	1.028	1.030	1.032
ν_{L2} (mm)	8.424	8.510	8.594	8.677	7.930	1.062	1.073	1.084	1.094

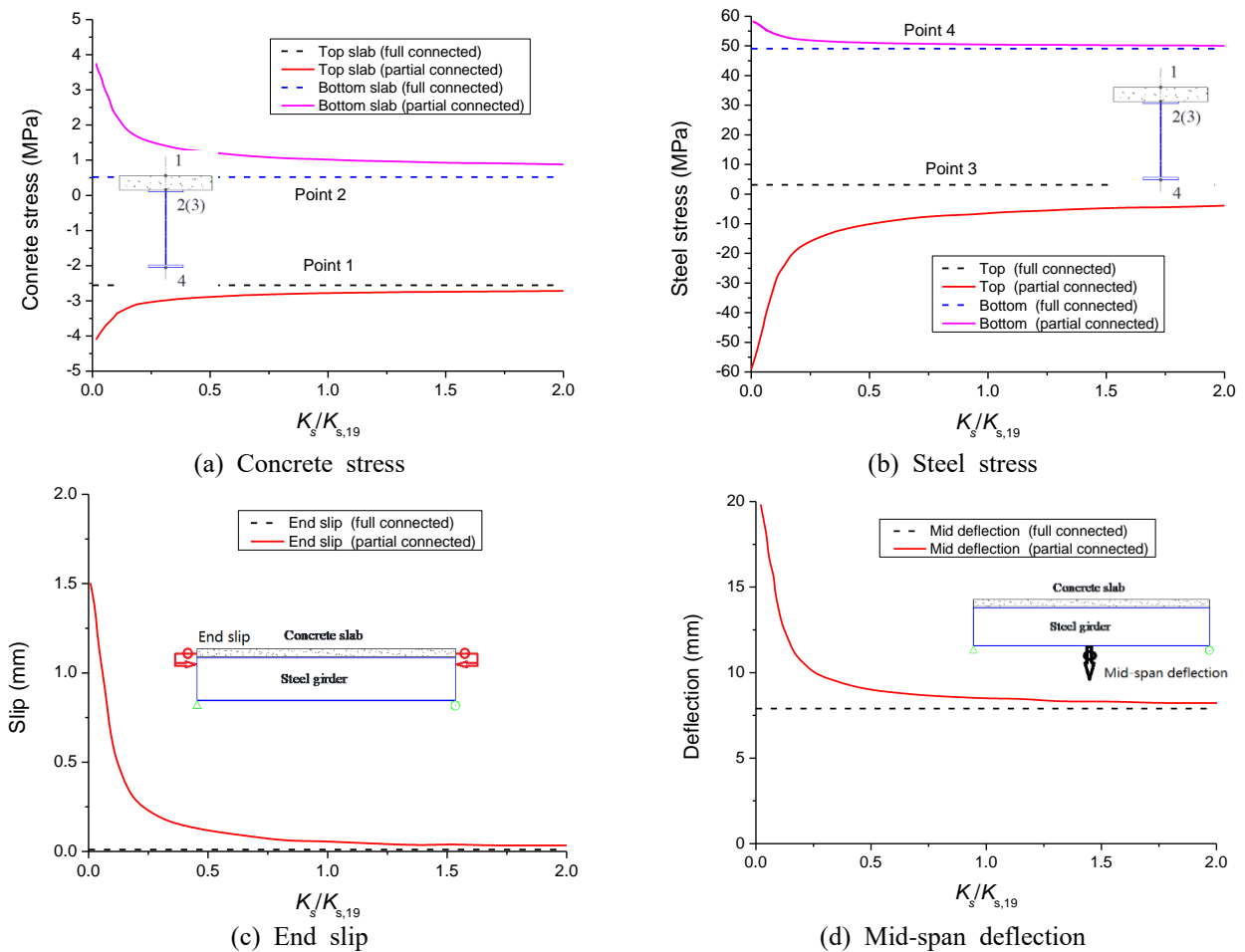


Fig. 11 Effect of shear stiffness under concentrated loading

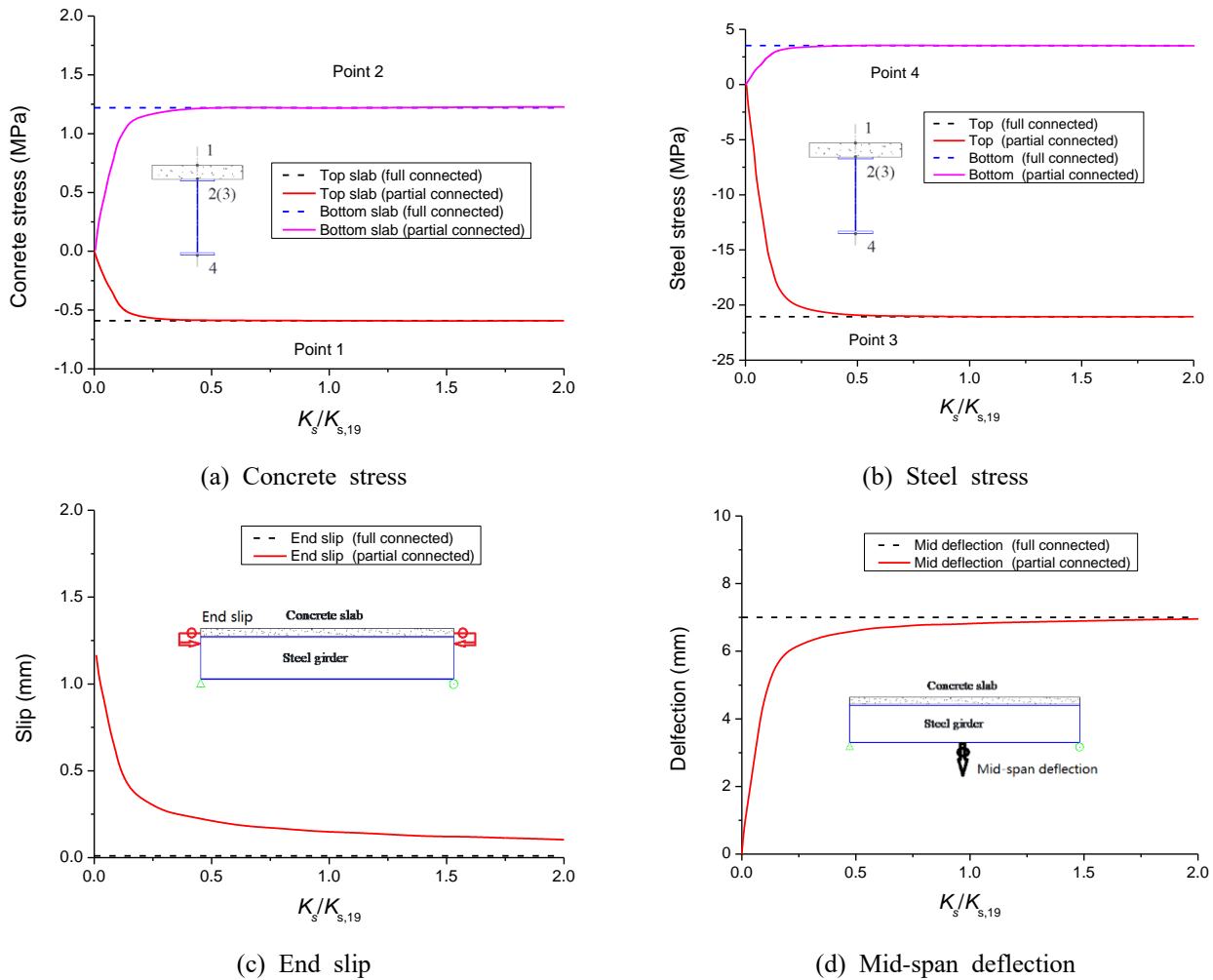


Fig. 12 Effect of shear stiffness under temperature difference loading

As the increasing of stud diameter, the shear stiffness at corresponding arrangement of studs decrease gradually, and the differences of stress and deflection between partially connection and fully connection become larger. For example, when installation of 19 mm-studs, the difference of σ_{c1} , σ_{c2} , σ_{s3} , v_{s4} and $y_{L/2}$ between partially connection and fully connection is 9.0%, 90.9%, 293.6%, 2.8% and 7.3%, respectively. The difference of stress at steel-concrete interface is obvious. It should be noted that although the difference of stress σ_{s3} is large, the stress level is very low, which can be ignored in compression with the yield stress of steel. Although the value of stress σ_{c2} is small, but is in tensile for concrete, which should be pay more attention. The difference of stress and deflection induced by concentrated loading is larger than that by uniform distributed loading, under the condition of adopting the same shear stiffness.

Under concentrated loading, in order to limit the difference of stress between partially connection and fully connection less than 5%, the shear stiffness should be more than 4.16×10^6 kN/m²; while to limit the difference of deflection less than 5%, the value should be more than 1.95×10^6 kN/m².

4.3.3 Under temperature difference loading

The temperature difference between concrete slab and steel beam is assumed to be -15°C . Fig. 12 and Table 4 show the effects of shear stiffness on the normal stress on top (σ_{c1}) and bottom (σ_{c2}) surface of concrete slab, normal stress on top (σ_{s3}) and bottom (σ_{s4}) surface of steel beam, deflection at middle span ($y_{L/2}$), and relative slip at end section. Similar to that under uniform distributed loading, when the shear stiffness is small, the effects on the stress, deflection and slip is significant, as the increasing of shear stiffness, the effects reduce gradually, and the stress, deflection and slip at partial connected condition tend to be those at full connected condition under temperature difference loading is faster than that under uniform distributed loading.

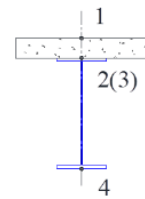
As the increasing of stud diameter, the shear stiffness at corresponding arrangement of studs decrease gradually, and the differences of stress and deflection between partially connection and fully connection become larger. For example, when installation of 19 mm-studs, the difference of σ_{c1} , σ_{c2} , σ_{s3} , v_{s4} and $y_{L/2}$ between partially connection and fully connection is 0.1%, 0%, 0.1%, 0.1% and 2.9%, respectively. All the differences are less than 5%, which can

Table 4 Structural response under temperature difference loading

Item	Partially connection-stud diameter				Fully connection	Partially connection/ Fully connection			
	16 mm	19 mm	22 mm	25 mm		16 mm	19 mm	22 mm	25 mm
σ_{c1} (MPa)	-0.593	-0.593	-0.593	-0.592	-0.593	1.000	0.999	0.999	0.999
σ_{c2} (MPa)	1.224	1.223	1.223	1.222	1.224	1.000	1.000	0.999	0.999
σ_{s3} (MPa)	-21.057	-21.051	-21.043	-21.031	-21.062	1.000	0.999	0.999	0.999
σ_{s4} (MPa)	3.528	3.527	3.525	3.523	3.529	1.000	0.999	0.999	0.999
$y_{L/2}$ (mm)	6.850	6.817	6.785	6.753	7.022	0.975	0.971	0.966	0.962

Table 5 Dimensions of four composite girders (unit: mm)

Components	Girder A	Girder B	Girder C	Girder D
Concrete slab	200×1800	240×2400	250×3000	260×3600
Top steel flange	16×200	20×300	24×500	28×600
Steel web	8×368	12×500	16×1352	20×1884
Bottom steel flange	16×250	20×400	24×600	28×800
Girder height	600	840	1650	2160
Girder span	12000	16800	33000	43200



be ignored. The difference of stress and deflection induced by temperature difference loading is much less than that by uniform distributed loading, under the condition of adopting the same shear stiffness. Therefore, the reaction of composite girder subjected to temperature difference or shrinkage can be calculated on the assumption that steel beam and concrete slab is fully connected.

Under temperature difference loading, in order to limit the difference of stress between partially connection and fully connection less than 5%, the shear stiffness should be more than $0.26 \times 10^6 \text{ kN/m}^2$; while to limit the difference of deflection less than 5%, the value should be more than $0.76 \times 10^6 \text{ kN/m}^2$.

4.4 The effect of shear stiffness for different composite girders

Generally, the effects of shear stiffness on the structural behaviors of steel-concrete girder depend on the geometric properties of composite girder (i.e., the span and cross-section). In bridge structure, the dimension of section is related to the span of composite girder, the height of the cross-section and the thickness of plate increase as the increase of the span. Therefore, this section will explore the influence of shear stiffness on the elastic behavior of composite girder with different geometry. For the convenience of comparison, the ratio of height to span of composite girder keep the same as 1/20, and the dimensions of four composite girders are shown in Table 5.

Fig. 13 shows the effects of shear stiffness on structural behaviors of steel-concrete girders with different dimensions. The parameters α_{c1} , α_{s4} and α_y are the difference ratio of stress at top concrete slab and bottom steel flange, deflection at mid-span under condition of partial connection to that under full connection. From girders A to D, using

19 mm-studs, the difference ratio of stress at top concrete slab is 0.127, 0.088, 0.011 and 0.02178, respectively, while the difference ratio of stress at bottom steel flange is 0.016, 0.027, 0.030 and 0.016, respectively, the difference ratio of deflection at mid-span is 0.093, 0.070, 0.036 and 0.026, respectively.

It can be found that the difference ratio of stress (α_{c1} , α_{s4}) and deflection (α_y) show different change rules. The difference ratio of stress at top concrete slab and bottom steel flange did not show a consistent rule with the increase of composite girder size. Because the calculation of stress depends not only on the overall rigidity of composite girder, but also on the relative rigidity of concrete slab and steel beam. For composite girders with different sizes, the relative rigidity of concrete slab and steel beam changes irregularly. For large-size composite girders, the values of both difference ratio of stress and deflection are small when using 19-mm studs, which is less than 5%. Thus, the calculation error of the stress for large-size composite girders is smaller than that for small-size composite girders based on the assumption of full connection. For the difference ratio of deflection (α_y), it mainly depends on the span and flexural rigidity of composite girder. With the increase of girder sizes, the flexural rigidity and span also monotonically increases, so the influence of connection's shear stiffness for different girder sizes on the deflection of composite girder shows a certain change rule. With the increase of girder sizes, the difference ratio of mid-span deflection decreases gradually, indicating that the calculation error for the large-sized composite girder is smaller than that for small-sized one based on the assumption of full connection.

For composite girders with different dimensions, in order to limit the difference of stress between partially connection and fully connection less than 5%, the shear

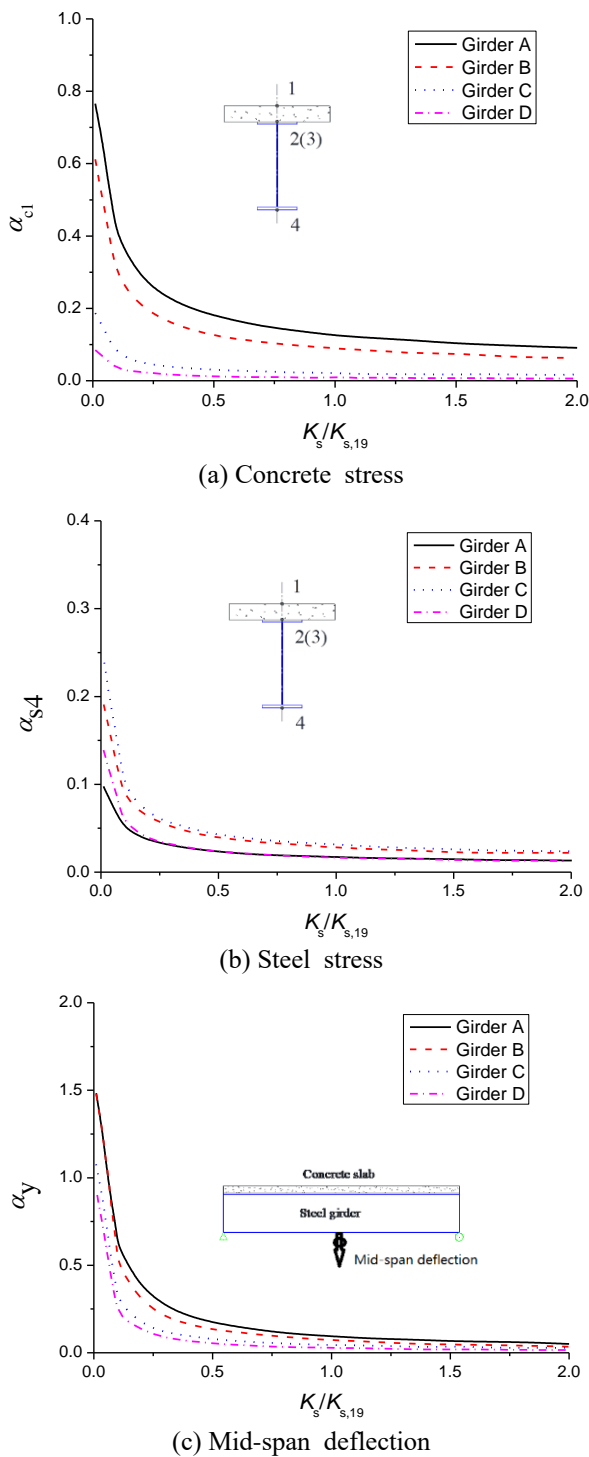


Fig. 13 Effect of shear stiffness for different composite girders

stiffness should be more than $5.68 \times 10^6 \text{ kN/m}^2$; while to limit the difference of deflection less than 5%, the value should be more than $1.74 \times 10^6 \text{ kN/m}^2$.

5. Conclusions

The shear stiffness of headed studs embedded in various types of concrete (NC, HPC, UHPC etc.) was investigated using totally 206 push-out tests from the literature, and a formulation for predicting shear stiffness of headed studs in elastic state was proposed. The effects of shear stiffness on the elastic behaviors of composite girders with different sizes and under different loading conditions were further analyzed. The following conclusions can be drawn from the present study:

- The shear stiffness of studs is defined as the secant stiffness of the load-slip curve at $0.5V_u$, because it can not only consists with the definition at slip of 0.2 mm for concrete strength less than 80 MPa, but also keeps the stud embedded in high strength concrete ($>80 \text{ MPa}$) still within elastic state. A new equation for shear stiffness was proposed based on the deformation and mechanic behavior of studs. The proposed formula indicates that the shear stiffness mainly depends on the stud diameter, and the elastic modulus of steel and concrete. And the shear stiffness predicted by the new formula agree well with test results for studs with a diameter ranging from 10 to 30 mm in the concrete with compressive strength ranging from 22.0 to 200.0 MPa.

- The equations for calculating the stress and deformation of simply supported composite girder considering the influence of connection's shear stiffness were derived under different loading conditions using classical linear partial-interaction theory. As the increasing of shear stiffness, the stress and deflection at the most unfavorable section under partial connected condition tend to be those under full connected condition, but the approaching speed decreases gradually.

- Using the same shear stiffness at steel-concrete interface, in term of the difference between the ultimate stress and the deflection of composite girder at mid-span for partial connected condition and those for fully connected condition, the value under the concentrated load is maximum, then under the uniform distrusted load, and under temperature difference (shrinkage) is the smallest. Under the action of temperature difference (shrinkage), the above-mentioned difference is less than 5% using common arrangement of headed studs, which can be designed as fully connection. However, under the action of concentrated load and uniform distrusted load, the difference is more than 5%, so the influence of connection's shear stiffness should be considered.

- In comparison with small-sized composite girders, the error for calculating the ultimate stress and the deflection at mid-span section based on the assumption of full connection is less for large-sized ones.

- For composite girders with different dimensions under different loading conditions, in order to limit the difference of ultimate stress between partially and fully connection less than 5%, the shear stiffness should be more than $5.68 \times 10^6 \text{ kN/m}^2$; while to limit the difference of deflection less than 5%, the value should be more than $1.95 \times 10^6 \text{ kN/m}^2$. The control factor should be the difference of ultimate stress at the most unfavorable section.

• On the premise of meeting the requirement of longitudinal shear force at steel-concrete interface, the arrangement of small-diameter headed studs provides more shear stiffness, results in less error for calculating the ultimate stress and the deflection at mid-span section based on the assumption of full connection.

Acknowledgments

The authors gratefully acknowledge the financial support provided by the National Nature Science Foundations of China (51978081, 51778069, 51708047), Horizon 2020- Marie Skłodowska-Curie Individual Fellowship of European Commission (REUSE: 793787), The Scientific Research Foundation of Hunan Provincial Education Department (18A131), Key Discipline Fund Project of Civil Engineering of Changsha University of Sciences and Technology (18ZDXK06).

References

- American Association of State Highway and Transportation Officials (AASHTO) (2014), AASHTO LRFD bridge design specifications. AASHTO, Washington DC, USA.
- An, L. and Cederwall, K. (1996), "Push-out tests on studs in high strength and normal strength concrete", *J. Constr. Steel Res.*, **36**(1), 15-29. [https://doi.org/10.1016/0143-974X\(94\)00036-H](https://doi.org/10.1016/0143-974X(94)00036-H).
- ANSI/AISC 360-05 (2005), *Specification for Structural Steel Buildings*. American Institute of Steel Construction.
- Badie, S.S., Tadros, M.K., Kakish, H.F., Splittgerber, D.L. and Baishya, M. C. (2002), "Large shear studs for composite action in steel bridge girders", *J. Bridge Eng.*, **7**(3), 195-203. [https://doi.org/10.1061/\(ASCE\)1084-0702\(2002\)7:3\(195\)](https://doi.org/10.1061/(ASCE)1084-0702(2002)7:3(195)).
- British Standard Institution (BSI) (1978), *Steel, Concrete and Composite Bridges, Part 3: Code of Practice for Design of Steel Bridges*. BS5400, British Standard Institution, London, UK.
- Cao, J., Shao, X., Deng, L. and Gan, Y. (2017), "Static and fatigue behavior of short-headed studs embedded in a thin ultra high performance concrete layer", *J. Bridge Eng. ASCE*, **22**(5), 04017005. [https://doi.org/10.1061/\(ASCE\)BE.1943-5592.0001031](https://doi.org/10.1061/(ASCE)BE.1943-5592.0001031).
- Comite Européen de Normalisation (CEN) (2005), Eurocode 4: Design of Composite Steel and Concrete Structures – Part 2: General Rules and Rules for Bridges. EN 1994-2, Brussels, Belgium.
- Chen, S. (2005), "Experimental study of prestressed steel-concrete composite beams with external tendons for negative moments", *J. Constr. Steel Res.*, **61**(12), 1613-1630. <https://doi.org/10.1016/j.jcsr.2005.05.005>.
- Colajanni, P., La Mendola, L. and Monaco, A. (2014), "Stress transfer mechanism investigation in hybrid steel trussed-concrete beams by push-out tests", *J. Constr. Steel Res.*, **95**, 56-70. <https://doi.org/10.1016/j.jcsr.2013.11.025>.
- Davies, C. (1967), "Small-scale push-out tests on welded stud shear connectors", *Concrete*, **1**(9), 311-316.
- Dogan, O. and Roberts, T.M. (2012), "Fatigue performance and stiffness variation of stud connectors in steel-concrete-steel sandwich systems", *J. Constr. Steel Res.*, **70**, 86-92. <https://doi.org/10.1016/j.jcsr.2011.08.013>.
- Dominic, K., Kay, W. and Zaghi, A.E. (2018), "Push-out behavior of headed shear studs welded on thin plates and embedded in UHPC", *Eng. Struct.*, **173**, 429-441. <https://doi.org/10.1016/j.engstruct.2018.07.013>.
- Gattesco, N., Giuriani, E. and Gubana, A. (1997), "Low-cycle fatigue test on stud shear connectors", *J. Struct. Eng. - ASCE*, **123**(2), 145-50. [https://doi.org/10.1061/\(ASCE\)0733-9445\(1997\)123:2\(145\)](https://doi.org/10.1061/(ASCE)0733-9445(1997)123:2(145)).
- Han, Q., Wang, Y., Xu, J. and Xing, Y. (2015), "Static behavior of stud shear connectors in elastic concrete-steel composite beams", *J. Constr. Steel Res.*, **113**, 115-26. <https://doi.org/10.1016/j.jcsr.2015.06.006>.
- Han, Q., Wang, Y., Xu, J. and Xing, Y. (2017), "Numerical analysis on shear stud in push-out test with crumb rubber concrete", *J. Constr. Steel Res.*, **130**, 148-158. <https://doi.org/10.1016/j.jcsr.2016.12.008>.
- He, J., Liu, Y., Chen, A. and Yoda, T. (2010), "Experimental study on inelastic mechanical behaviour of composite girders under hogging moment", *J. Constr. Steel Res.*, **66**(1), 37-52. <https://doi.org/10.1016/j.jcsr.2009.07.005>.
- He, J., Liu, Y., Chen, A., Wang, D. and Yoda, T. (2014), "Bending behavior of concrete-encased composite I-girder with corrugated steel web", *Thin-Wall. Struct.*, **74**, 70-84. <https://doi.org/10.1016/j.tws.2013.08.003>.
- He, J., Wang, S., Liu, Y., Lyu, Z. and Li, C. (2017), "Mechanical behavior of partially encased composite girder with corrugated steel web: interaction of shear and bending", *Engineering*, **3**, 806-816. <https://doi.org/10.1016/j.eng.2017.11.005>.
- He, J., Liu, Y., Wang, S., Xin, H., Chen, H. and Ma, C. (2019), "Experimental study on structural performance of prefabricated composite box girder with corrugated webs and steel tube slab", *J. Bridge Eng. ASCE*, **24**(6), 04019047. [https://doi.org/10.1061/\(ASCE\)BE.1943-5592.0001405](https://doi.org/10.1061/(ASCE)BE.1943-5592.0001405).
- He, J., Li, X., Li, C., Correia, J., Xin, H. and Zhou, M. (2020a), "A novel asynchronous-pouring-construction technology for prestressed concrete box girder bridges with corrugated steel webs", *Structures*, **27**, 1940-1950. <https://doi.org/10.1016/j.istruc.2020.07.077>.
- He, J., Wang, S., Liu, Y., Wang, D. and Xin, H. (2020b), "Shear behavior of steel I-girder with stiffened corrugated web, Part II: Numerical study", *Thin-Wall. Struct.*, **147**, <https://doi.org/10.1016/j.tws.2019.02.023>.
- JSCE (2009), *Standard specifications for hybrid structures*, Japan Society of Civil Engineers, Tokyo.
- JTG/T D64-01-2015, *Specifications for Design and Construction of Highway Steel-concrete Composite Bridge*, China Communications Press, China.
- Johnson R.P. (2008). *Composite structures of steel and concrete: Beams, slabs and frames for buildings*, Third Edition. Oxford, Blackwell publishing Ltd.
- Johnson, R.P. and May, I.M. (1975), "Partial-interaction design of composite beams", *The Structural Engineer*, **8**(53), 305-311.
- Kim, J.S., Kwark, J. and Joh, C. (2015), "Headed stud shear connector for thin ultra high performance concrete bridge deck", *J. Constr. Steel Res.*, **108**, 23-30. <https://doi.org/10.1016/j.jcsr.2015.02.001>.
- Lam, D. and El-Lobody, E. (2005), "Behavior of headed stud shear connectors in composite beam", *J. Struct. Eng. - ASCE*, **131**(1), 96-107. [https://doi.org/10.1061/\(ASCE\)0733-9445\(2005\)131:1\(96\)](https://doi.org/10.1061/(ASCE)0733-9445(2005)131:1(96)).
- Lee, P.G., Shim, C.S. and Chang, S.P. (2005), "Static and fatigue behavior of large stud shear connectors for steel-concrete composite bridges", *J. Constr. Steel Res.*, **61**(9), 1270-1285. <https://doi.org/10.1016/j.jcsr.2005.01.007>.
- Lin, W., Yoda, T. and Taniguchi, N. (2014a), "Application of SFRC in steel-concrete composite beams subjected to hogging moment", *J. Constr. Steel Res.*, **101**, 175-83. <https://doi.org/10.1016/j.jcsr.2014.05.008>.
- Lin, W., Yoda, T., Taniguchi, N., Kasano, H. and He, J. (2014b), "Mechanical performance of steel-concrete composite beams subjected to a hogging moment", *J. Struct. Eng. -ASCE*, **140**(1),

04013031. [https://doi.org/10.1061/\(ASCE\)ST.1943-541X.0000800](https://doi.org/10.1061/(ASCE)ST.1943-541X.0000800).
- Lin, Z. (2016), Design method of stud connections between concrete slabs and steel girders in steel-concrete composite bridges, Doctoral Thesis, Tongji University, Shanghai, China (in Chinese).
- Lin, Z., Liu, Y. and He, J. (2014), "Behavior of stud connectors under combined shear and tension loads", *Eng. Struct.*, **81**, 362-376. <https://doi.org/10.1016/j.engstruct.2014.10.016>.
- Lin, Z., Liu, Y. and He, J. (2015), "Static behaviour of lying multi-stud connectors in cable-pylon anchorage zone", *Steel Compos. Struct.*, **18**(6), 1369-1389. <https://doi.org/10.12989/scs.2015.18.6.1369>.
- Lin, Z., Liu, Y. and Roeder, C.W. (2016), "Behavior of stud connections between concrete slabs and steel girders under transverse bending moment", *Eng. Struct.*, **117**, 130-44. <https://doi.org/10.1016/j.engstruct.2016.03.014>.
- Liu, Y., Zhang, Q., Bao, Y. and Bu, Y. (2018), "Static and fatigue push-out tests of short headed shear studs embedded in Engineered Cementitious Composites (ECC)", *Eng. Struct.*, **182**, 29-38. <https://doi.org/10.1016/j.engstruct.2018.12.068>.
- Luo, Y., Hoki, K., Hayashi, K. and Nakashima, M. (2016), "Behavior and strength of headed stud-SFRCC shear connection. I: experimental study", *J. Struct. Eng.*, **142**(2), 1-10. [https://doi.org/10.1061/\(ASCE\)ST.1943-541X.0001363](https://doi.org/10.1061/(ASCE)ST.1943-541X.0001363)
- Oehlers, D.J. and Bradford, M.A. (1999), Elementary behaviour of composite steel and concrete structural members. Oxford: Butterworths-Heinemann.
- Oehlers, D.J. and Coughlan, C.G. (1986), "The shear stiffness of stud shear connections in composite beams", *J. Constr. Steel Res.*, **6**(4), 273-284. [https://doi.org/10.1016/0143-974X\(86\)90008-8](https://doi.org/10.1016/0143-974X(86)90008-8).
- Ollgaard, J.G., Slutter, R.G. and Fisher, J.W. (1971), "Shear strength of stud connectors in light weight and normal weight concrete", *Eng. J.*, **8**, 55-64.
- Qi, J., Hu, Y., Wang, J. and Li, W. (2019), "Behavior and strength of headed stud shear connectors in ultra-high performance concrete of composite bridges", *Front. Struct. Civ. Eng.*, **13**(5), 1138-1149. <https://doi.org/10.1007/s11709-019-0542-6>.
- Pallarés, L. and Hajjar, J.F. (2010), "Headed steel stud anchors in composite structures, Part I: Shear", *J. Constr. Steel Res.*, **66**(2), 198-212. <https://doi.org/10.1016/j.jcsr.2009.08.009>.
- Ranzi, G., Leoni, G. and Zandonini, R. (2013), "State of the art on the time-dependent behaviour of composite steel-concrete structures", *J. Constr. Steel Res.*, **80**, 252-263. <https://doi.org/10.1016/j.jcsr.2012.08.005>.
- Shim, C.S., Lee, P.G. and Yoon, T.Y. (2004), "Static behavior of large stud shear connectors", *Eng. Struct.*, **26**(12), 1853-1860. <https://doi.org/10.1016/j.engstruct.2004.07.011>.
- Spacone, E. and El-Tawil, S. (2004), "Nonlinear analysis of steel concrete composite structures: state of the art", *J. Struct. Eng.*, **130**, 159-168. [https://doi.org/10.1061/\(ASCE\)0733-9445\(2004\)130:2\(159\)](https://doi.org/10.1061/(ASCE)0733-9445(2004)130:2(159)).
- Spremic, M., Markovic, Z. and Veljkovic, M. (2013), "Push-out experiments of headed shear studs in group arrangements" *Adv. Steel Constr.*, **9**(2), 139-160. <https://doi.org/10.18057/IJASC.2013.9.2.4>.
- Spremic, M., Pavlovic, M., Markovic, Z., Veljkovic, M. and Budjevac, D. (2018), "FE validation of the equivalent diameter calculation model for grouped headed studs", *Steel Compos. Struct.*, **26**(3), 375-386. <https://doi.org/10.12989/scs.2018.26.3.375>.
- Suwaed A.S.H. and Karavasilis T.L. (2018), "Removable shear connector for steel-concrete composite bridges", *Steel Compos. Struct.*, **29**(1), 107-123. <https://doi.org/10.12989/scs.2018.29.1.107>.
- Tian, Q. and Du, X. (2016), "Short stud push-out test study of high performance concrete composite pavement", *Bridge Constr.*, **46**(1), 40-46 (in Chinese).
- Valente, I.B. and Cruz, P.J.S. (2009), "Experimental analysis of shear connection between steel and lightweight concrete", *J. Constr. Steel Res.*, **65**, 1954-1963. <https://doi.org/10.1016/j.jcsr.2009.06.001>.
- Viest, I.M. (1956), "Investigation of stud shear connectors for composite concrete and steel t-beams", *ACI J. Proceedings*, **52**(4), 875-892.
- Wang, J., Qi, J., Tong, T., Xu, Q. and Xiu, H. (2019), "Static behavior of large stud shear connectors in steel-UHPC composite structures", *Eng. Struct.*, **178**, 534-542. <https://doi.org/10.1016/j.engstruct.2018.07.058>.
- Wang, J. Xu, Q., Yao, Y., Qi, J. and Xiu, H. (2018), "Static behavior of grouped large headed stud-UHPC shear connectors in composite structures", *Compos. Struct.*, **206**, 202-214. <https://doi.org/10.1016/j.compstruct.2018.08.038>.
- Wang, Q. (2013), Experimental research on mechanical behavior and design method of stud connectors. Doctoral Thesis, Tongji University, Shanghai, China (in Chinese).
- Wang, Y.C. (1998), "Deflection of steel-concrete composite beams with partial shear interaction", *J. Struct. Eng.*, **124**, 1159-1165. [http://dx.doi.org/10.1061/\(ASCE\)0733-9445\(1998\)124:10\(1159\)](http://dx.doi.org/10.1061/(ASCE)0733-9445(1998)124:10(1159)).
- Xu, C., Su, Q. and Masuya, H. (2017), "Static and fatigue performance of stud shear connector in steel fiber reinforced concrete", *Steel Compos. Struct.*, **24**(4), 467-479. <https://doi.org/10.12989/scs.2017.24.4.467>.
- Xu, C., Su, Q. and Masuya, H. (2018), "Static and fatigue behavior of the stud shear connector in lightweight concrete", *Int. J. Steel Struct.*, **18**, 569-581. <https://doi.org/10.1007/s13296-018-0014-1>.
- Xu, X., Liu, Y. and He, J. (2014), "Study on mechanical behavior of rubber-sleeved studs for steel and concrete composite structures", *Constr. Build. Mater.*, **53**, 533-546. <https://doi.org/10.1016/j.conbuildmat.2013.12.011>.
- Xu, X. and Liu, Y. (2016), "Analytical and numerical study of the shear stiffness of rubber-sleeved stud", *J. Constr. Steel Res.*, **123**, 68-78. <https://doi.org/10.1016/j.jcsr.2016.04.020>.
- Xu, X. and Liu, Y. (2019), "Analytical prediction of the deformation behavior of headed studs in monotonic push-out tests", *Adv. Struct. Eng.*, **22**(7), 1711-1726. <https://doi.org/10.1177/1369433218821750>.
- Xue, D., Liu, Y., Yu, Z. and He, J. (2012), "Static behavior of multi-stud shear connectors for steel-concrete composite bridge", *J. Constr. Steel Res.*, **74**(8), 1-7. <https://doi.org/10.1016/j.jcsr.2011.09.017>.
- Xue, W., Ding, M., Wang, H. and Luo, Z. (2008), "Static behavior and theoretical model of stud shear connectors", *J. Bridge Eng.*, **13**(6), 623-634. [https://doi.org/10.1061/\(ASCE\)1084-0702\(2008\)13:6\(623\)](https://doi.org/10.1061/(ASCE)1084-0702(2008)13:6(623)).
- Zhan, Y., Yin, C., Liu, F., Song, R., Deng, K. and Sun, J. (2020), "Push-out tests on headed studs and PBL shear connectors considering external pressure", *J. Bridge Eng.*, **25**(1), 04019125. [https://doi.org/10.1061/\(ASCE\)BE.1943-5592.0001506](https://doi.org/10.1061/(ASCE)BE.1943-5592.0001506).